






# Unsupervised Blind Joint Dereverberation and Room Acoustics Estimation with Diffusion Models

Jean-Marie Lemerrier\* , *Student Member, IEEE*, Eloi Moliner\* , Simon Welker , *Student Member, IEEE*, Vesa Välimäki , *Fellow, IEEE*, Timo Gerkmann , *Senior Member, IEEE*

**Abstract**—This paper presents an unsupervised method for single-channel blind dereverberation and room impulse response (RIR) estimation, called BUDDy. The algorithm is rooted in Bayesian posterior sampling: it combines a likelihood model enforcing fidelity to the reverberant measurement, and an anechoic speech prior implemented by an unconditional diffusion model. We design a parametric filter representing the RIR, with exponential decay for each frequency subband. Room acoustics estimation and speech dereverberation are jointly carried out, as the filter parameters are iteratively estimated and the speech utterance refined along the reverse diffusion trajectory. In a blind scenario where the room impulse response is unknown, BUDDy successfully performs speech dereverberation in various acoustic scenarios, significantly outperforming other blind unsupervised baselines. Unlike supervised methods, which often struggle to generalize, BUDDy seamlessly adapts to different acoustic conditions. This paper extends our previous work by offering new experimental results and insights into the algorithm’s performance and versatility. We first investigate the robustness of informed dereverberation methods to RIR estimation errors, to motivate the joint acoustic estimation and dereverberation paradigm. Then, we demonstrate the adaptability of our method to high-resolution singing voice dereverberation, study its performance in RIR estimation, and conduct subjective evaluation experiments to validate the perceptual quality of the results, among other contributions. Audio samples and code can be found online.<sup>1</sup>

**Index Terms**—Acoustics, diffusion models, reverberation, speech enhancement.

## I. INTRODUCTION

REVERBERATION is a natural phenomenon caused by acoustic waves propagating in a room and getting reflected by walls. Reverberation and particularly late reflections often degrade speech intelligibility and quality for normal listeners, and even more severely so for hearing-impaired listeners [1]. Therefore, many communication devices now include a dereverberation algorithm, which aims to recover the anechoic component of speech. This paper considers the scenario in which recordings from only one microphone are available, which is more challenging than a multi-channel scenario [2].

Traditional dereverberation algorithms operate in the time, spectral, or cepstral domain [3], leveraging statistical assump-

tions about the anechoic and reverberant signals [4] as well as properties of the reverberation signal model [5]. Two scenarios are considered for dereverberation, depending on the knowledge of the room acoustics represented by the room impulse response (RIR). Some methods tackle *informed* scenarios, where the RIR is known [5], [6], whereas other approaches consider *blind* scenarios where the RIR is unknown [7]–[11]. Informed dereverberation is naturally an easier task than blind dereverberation. However, knowing the RIR does not guarantee obtaining a stable and causal inverse filter in the single-channel case, since real-world RIRs are mixed-phase systems [12]. Using multiple microphones helps resolve this issue to some extent [2], but informed dereverberation methods generally exhibit other weaknesses such as a lack of robustness to RIR estimation errors [13]. Additionally, most scenarios in real-life applications are (at least partially) blind, as the RIR is either not measured beforehand, or only valid for a specific acoustic setting.

Data-driven approaches rely less on distributional assumptions than statistical methods but instead directly learn the signal properties and structures from data [14]. Among these, supervised predictive models are particularly popular for blind dereverberation: these range from time-frequency masking [15] and mapping [16] to algorithms operating on the cepstrum [17] or directly on the waveform [18], [19].

Generative modeling is another paradigm gaining a lot of interest in audio restoration tasks [20], including dereverberation. Generative models for speech dereverberation learn a parameterization of the posterior distribution of clean speech conditioned on reverberant speech. Diffusion models in particular [21]–[23] have been extensively investigated for such conditional generation task, leading to the introduction of diffusion-based blind supervised dereverberation algorithms [24], [25]. Still, the generalization ability of supervised approaches is limited by their design.

In contrast, unsupervised methods have been getting little visibility but boast interesting properties such as improved robustness to unseen acoustic conditions without the need for retraining. An unsupervised method for informed single-channel dereverberation based on diffusion models was proposed in our prior work [26]. That approach is based on Bayesian diffusion posterior sampling (DPS) [27], combining a diffusion-based anechoic speech prior and a Gaussian likelihood model for state-of-the-art informed dereverberation. However, as shown in this work, such an informed algorithm is sensitive to even small RIR estimation errors, rendering it impractical in real-life scenarios.

\*Equal contribution. Jean-Marie Lemerrier, Simon Welker and Timo Gerkmann are with the Signal Processing group at Universität Hamburg, Hamburg, Germany. Eloi Moliner and Vesa Välimäki are with the Acoustics Lab, Department of Information Communications Engineering, Aalto University, Espoo, Finland. The authors gratefully acknowledge the computing resources provided by both the Erlangen National High Performance Computing Center (NHR@FAU) of the Friedrich-Alexander-Universität Erlangen-Nürnberg (FAU) (NHR project F101AC1) and the Aalto Science-IT project.

<sup>1</sup>uhh.de/sp-inf-buddy

Related works in other signal processing domains have already considered blind inverse problems through the lens of posterior sampling with diffusion priors. For image deblurring, Chung et al. [28] propose to use an additional diffusion process dedicated to estimating the deblurring kernel, while Laroche et al. [29] adapts an expectation-maximization algorithm using a denoising regularization of the blurring kernel, and Sanghvi et al. [30] dedicates a non-blind solver to estimate a deblurred image at each diffusion step. For speech denoising, Nortier et al. [31] combine a noise model based on non-negative matrix factorization with a clean speech diffusion prior. Moliner et al. [32] address the problem of blind bandwidth extension by leveraging a diffusion prior and iteratively optimizing a parametric lowpass filter operator. Recent works adapt denoising diffusion restoration models (DDRM) [33] for singing voice dereverberation [34], [35], using an initialization provided by the weighted-prediction error (WPE) algorithm [7].

For speech dereverberation, a first generative model based on traditional Gaussian mixtures was proposed in [36]. Other works learn an anechoic speech prior via variational auto-encoding (VAE): the VAE-NMF method [37] models reverberation via non-negative matrix factorization and estimates its parameters with a Monte-Carlo method; the RVAE-EM model [38] adopts a maximum a posteriori perspective, combining a recurrent VAE prior with a Gaussian likelihood model. Unsupervised dereverberation with a non-generative prior has also been investigated in the multi-channel scenario [39].

This paper expands our prior work [40], where we designed a blind unsupervised dereverberation algorithm, extending [26] to the blind scenario. The resulting approach, called BUDDy, uses a model-based parametric subband filter with an exponential decay to approximate the RIR. BUDDy performs joint estimation of the RIR and the anechoic speech, leveraging the model-based parameterization as an acoustic prior and the diffusion model as a speech prior. We have shown previously [40] that BUDDy can successfully remove reverberation, and that it is robust to changes in acoustic conditions because of the lack of supervision during training. Therefore, BUDDy closes the performance gap between matched and mismatched acoustic conditions in comparison to diffusion-based supervised approaches [24], [25].

In this paper, we extend the experimental framework of our previous publication [40] with the following contributions:

- In Section II, we investigate the *robustness* of informed dereverberation approaches in partially blind scenarios. We highlight the limitations of these approaches when the RIR is perturbed with Gaussian noise or estimated blindly using a state-of-the-art RIR estimator [41].
- Section V-A extends the evaluation of BUDDy for speech dereverberation beyond instrumental metrics, including a *subjective listening test* and a set of *ablation studies*.
- Section V-B presents new experiments on applying BUDDy to *singing voice dereverberation* at a sampling rate of 44.1 kHz, which is higher compared to the 16-kHz sampling rate used in our speech experiments [40]. The results, which also include a subjective listening test, indicate that our method significantly outperforms existing unsupervised state-of-the-art approaches and performs

comparably to a supervised adaptation of the proposed method.

- Finally, Section V-C assesses BUDDy’s performance in *RIR estimation* against a state-of-the-art supervised estimator [41]. We use frequency-wise acoustic descriptors to evaluate the accuracy of BUDDy on reverberation time and clarity.

We organize the paper as follows. Section II reports on the robustness of RIR-informed methods, providing context for the proposed approach. In Section III, we introduce diffusion-based generative models and posterior sampling methods for dereverberation using diffusion priors as proposed in previous work [26]. Then in Section IV, we introduce our blind unsupervised dereverberation method BUDDy [40]. The experiments and results mentioned above are presented in Section V. Lastly, Section VI concludes the paper.

## II. ROBUSTNESS OF RIR-INFORMED METHODS IN PARTIALLY BLIND SCENARIOS

We consider dereverberation under the prism of inverse problem solving: we wish to retrieve the anechoic utterance waveform  $\mathbf{x}_0 \in \mathbb{R}^L$ , where  $L$  is the speech utterance length, given the reverberant measurement  $\mathbf{y}$ . Reverberation is often modelled as a convolution between the anechoic speech with a RIR  $\mathbf{h} \in \mathbb{R}^{L_h}$ , such that  $\mathbf{y} = \mathbf{h} * \mathbf{x}_0$ , where  $*$  is the discrete convolution operator in the time domain, resulting in  $\mathbf{y} \in \mathbb{R}^{L+L_h-1}$ .

Informed dereverberation algorithms such as [5], [26] assume complete knowledge of the room acoustics as provided by the RIR  $\mathbf{h}$ . However, as pointed out in Section I, even if the RIR is perfectly known, single channel dereverberation is not trivial as RIRs represent mixed-phase systems such that causal and stable inverse filters do not exist [12]. In practical applications, the RIR is often unknown, and even when it can be estimated, there are typically estimation errors making the task of robust single channel dereverberation even harder. Before delving into blind dereverberation, which is the main focus of this paper, we first examine and demonstrate the sensitivity of informed dereverberation methods in such *partially blind* scenarios, i.e., when RIRs are known up to estimation errors.

We investigate here two methods, the first of which is our prior work InfDerevDPS [26], which is based on Bayesian diffusion posterior sampling (DPS) [27]. InfDerevDPS combines a diffusion-based anechoic speech prior and a Gaussian likelihood model which measures the adherence of the current estimate to the reverberant utterance, given the reverberation operator. The diffusion-based speech prior and sampling technique for InfDerevDPS are presented in Section III-B hereafter. The second method RIF+Post [5] performs regularized inverse filtering in the Fourier domain, followed by traditional speech enhancement.

We start studying the case where the oracle RIR is corrupted by Gaussian noise. The results displayed in Fig. 1 indicate that the performance of both the diffusion-based and the traditional method dwindles as the noise power increases. This suggests that informed methods have very limited robustness to errors

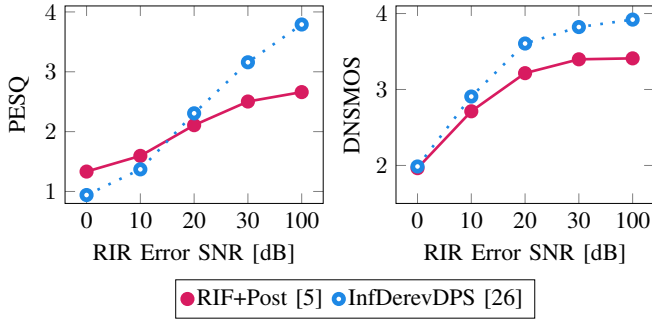


Fig. 1: Robustness of informed dereverberation approaches with respect to normally distributed errors in the RIR.

TABLE I: Dereverberation results on matched reverberant VCTK dataset. We indicate for each method in the table if it operates in a blind scenario.

Method	Blind	DNS-MOS	PESQ
Reverberant	-	$3.14 \pm 0.52$	$1.61 \pm 0.37$
RIF+Post [5]	✗	$3.41 \pm 0.47$	$2.66 \pm 0.40$
InfDerevDPS [26]	✗	$3.91 \pm 0.33$	$3.95 \pm 0.42$
FiNS/RIF+Post [5], [41]	✓	$2.18 \pm 0.38$	$1.33 \pm 0.19$
FiNS/InfDerevDPS [26], [41]	✓	$2.19 \pm 0.43$	$1.32 \pm 0.18$
BUDDy (ours) [40]	✓	<b><math>3.76 \pm 0.41</math></b>	<b><math>2.30 \pm 0.53</math></b>

in the provided RIR. This is problematic since perfect sample-wise estimation of RIRs is an arduous problem, given the statistical nature of RIRs [11].

We now shift to a more practical scenario where the RIR is estimated from the reverberant speech only by a DNN-based estimator. In particular, we employ FiNS [41], a state-of-the-art supervised RIR estimator which obtains RIR estimates based on the reverberant utterance (see Section V-C1 for details). We compare in Table I results where the RIR is perfectly known (i.e. informed scenario) versus when it is estimated by FiNS (i.e. partially blind). The acoustic conditions in the considered evaluation set match those of the training set. Therefore, since FiNS was trained in a supervised fashion using paired reverberant/RIR data, it is expected to perform well on such conditions. Indeed, through informal listening, we notice that FiNS produces perceptually reasonable RIR estimates. Yet, the dereverberation performance of both InfDerevDPS and RIF+Post is poor when the RIR is estimated with FiNS [41], as opposed to when the RIR is perfectly known. This shows the limited robustness of these informed methods, and suggests that in such blind case the RIR should be jointly estimated with the anechoic speech. This is the paradigm followed by our method BUDDy, which we will introduce in the next sections.

### III. INFORMED DIFFUSION-BASED DEREVERBERATION

This section introduces diffusion models, a class of generative models that form the foundation of the proposed method. It also explores their application in solving inverse problems, specifically highlighting their use in informed dereverberation.

#### A. Diffusion-Based Generative Models

Diffusion models [22], [42] have achieved remarkable success across various domains, including speech [43]. They break down the problem of generating high-dimensional complex data into a series of easier denoising tasks. Training a diffusion model first requires defining a *forward process*, which gradually adds noise to data points, turning the target data distribution into a tractable Gaussian distribution. Conversely, data generation is accomplished by reversing the corruption process. First, an initial sample is drawn from a Gaussian distribution, and then the model iteratively removes noise until a clean sample from the target distribution emerges.

The *reverse process*, which defines a transport between a Gaussian prior distribution and a target data distribution  $p_{\text{data}}$ , can be characterized by the *probability flow* ordinary differential equation (ODE):

$$d\mathbf{x}_\tau = [\mathbf{f}(\mathbf{x}_\tau, \tau) - \frac{1}{2}g^2(\tau)\nabla_{\mathbf{x}_\tau} \log p(\mathbf{x}_\tau)]d\tau, \quad (1)$$

where diffusion time  $\tau$  flows in reverse from  $\tau = T$  to  $\tau = T_{\min} \ll T$ . The diffusion state  $\mathbf{x}_\tau \in \mathbb{R}^L$  starts from the initial condition  $\mathbf{x}_T \in \mathbb{R}^L$  and ends at  $\mathbf{x}_0 \in \mathbb{R}^L \sim p_{\text{data}}$ , where  $L$  is the length of the time-domain speech utterance. We adopt the parameterization proposed by Karras et al. [44], which defines the *drift* and *diffusion* parameters as  $f(\mathbf{x}_\tau, \tau) = 0$  and  $g(\tau) = \sqrt{2\tau}$ , respectively. Similarly, we adopt  $\sigma(\tau) = \tau$  as the noise schedule which defines the so-called *transition kernel* i.e. the marginal density of the forward process:

$$q_\tau(\mathbf{x}_\tau|\mathbf{x}_0) = \mathcal{N}(\mathbf{x}_\tau, \sigma^2(\tau)\mathbf{I}), \quad (2)$$

where  $\mathbf{I} \in \mathbb{R}^{L \times L}$  is the identity matrix. The *score function*  $\nabla_{\mathbf{x}_\tau} \log p(\mathbf{x}_\tau)$  indicates the direction of maximum data likelihood. In practice, it is intractable and we need to estimate it with a *score model*  $\mathbf{s}_\theta(\mathbf{x}_\tau, \tau)$  parameterized with a deep neural network (DNN). Vincent et al. have shown that the score model  $\mathbf{s}_\theta(\mathbf{x}_\tau, \tau)$  can be optimized using denoising score matching, i.e. matching the score of the Gaussian transition kernel  $q_\tau(\mathbf{x}_\tau|\mathbf{x}_0)$  instead of the score of the unknown probability  $p(\mathbf{x}_\tau)$  [45]. The score of the transition kernel  $q_\tau(\mathbf{x}_\tau|\mathbf{x}_0)$  can be obtained from (2) as:

$$\nabla_{\mathbf{x}_\tau} q_\tau(\mathbf{x}_\tau|\mathbf{x}_0) = \frac{\mathbf{x}_\tau - \boldsymbol{\mu}(\mathbf{x}_0, \tau)}{\sigma(\tau)^2}. \quad (3)$$

The score model  $\mathbf{s}_\theta$  is therefore trained using the denoising score-matching objective: [45]

$$\mathbb{E}_{\substack{\tau \sim \mathcal{U}(T_{\min}, T_{\max}) \\ \mathbf{x}_0 \sim p_{\text{data}} \\ \mathbf{x}_\tau \sim q_\tau(\mathbf{x}_\tau|\mathbf{x}_0)}} \left[ \lambda(\tau) \left\| \mathbf{s}_\theta(\mathbf{x}_\tau, \tau) - \frac{\mathbf{x}_\tau - \boldsymbol{\mu}(\mathbf{x}_0, \tau)}{\sigma^2(\tau)} \right\|_2^2 \right], \quad (4)$$

where first a diffusion index  $\tau$  is randomly sampled between extremal times  $T_{\min}$  and  $T_{\max} > T$ , a data point  $\mathbf{x}_0$  is sampled in the training set, and the corresponding diffusion state  $\mathbf{x}_\tau$  is obtained from the transition kernel in (2). In practice, we use the same pre-conditioning for  $\mathbf{s}_\theta(\mathbf{x}_\tau, \tau)$  and same loss weighting  $\lambda(\cdot)$  as in Karras et al. (see [44] for details).

**Algorithm 1** Reverberation Operator  $\mathcal{A}_\psi(\cdot)$ 


---

**Require:** parameters  $\psi$ , speech estimate  $\hat{\mathbf{x}}_0$

$\{\Phi, (w_b, \alpha_b)_{b=1, \dots, B}\} \leftarrow \psi$  ▷ Parameter set

$\mathbf{A}'_{n,b} \leftarrow w_b \cdot e^{-\alpha_b n}$  ▷ Exponential decay model

$\mathbf{A} \leftarrow \exp\{\text{lerp}(\log \mathbf{A}')\}$  ▷ Frequency interpolation

$\mathbf{H} = \mathbf{A} e^{j\Phi}$

$\bar{\mathbf{H}} = \text{STFT}(\delta_d \oplus \mathcal{P}_{\min}(\text{iSTFT}(\mathbf{H})))$  ▷ Projection step

$\hat{\mathbf{X}} = \text{STFT}(\hat{\mathbf{x}}_0)$

$\hat{\mathbf{Y}}_{m,k} \leftarrow \sum_{n=0}^{N_h} \bar{\mathbf{H}}_{n,k} \hat{\mathbf{X}}_{m-n,k}$  ▷ Subband convolution

**return**  $\text{iSTFT}(\hat{\mathbf{Y}})$

---

**B. Diffusion Posterior Sampling for Dereverberation**

We discuss in this section how diffusion priors can be adapted in order to solve inverse problems. While some traditional methods derive maximum a posteriori estimators for blind dereverberation [9]–[11], we exploit the generative nature of diffusion models to solve this inverse problem using posterior sampling. Assuming for now that the RIR  $\mathbf{h}$  is known, we attempt to sample from the posterior distribution of the anechoic speech given the measurement and the RIR  $p(\mathbf{x}_0|\mathbf{y}, \mathbf{h})$ . This is achieved by solving the probability flow ODE (1), replacing the score function  $\nabla_{\mathbf{x}_\tau} \log p(\mathbf{x}_\tau)$  by the *posterior score*  $\nabla_{\mathbf{x}_\tau} \log p(\mathbf{x}_\tau|\mathbf{y}, \mathbf{h})$  [23]. The posterior score is obtained through Bayes' rule as:

$$\nabla_{\mathbf{x}_\tau} \log p(\mathbf{x}_\tau|\mathbf{y}, \mathbf{h}) = \nabla_{\mathbf{x}_\tau} \log p(\mathbf{x}_\tau) + \nabla_{\mathbf{x}_\tau} \log p(\mathbf{y}|\mathbf{x}_\tau, \mathbf{h}). \quad (5)$$

The first term, or *prior score*, is directly obtained via the score model  $\mathbf{s}_\theta(\mathbf{x}_\tau, \tau)$ . The likelihood score  $\nabla_{\mathbf{x}_\tau} \log p(\mathbf{y}|\mathbf{x}_\tau, \mathbf{h})$  is in general intractable for  $\tau > 0$ . As in [27], we employ an estimate of  $\mathbf{x}_0$ , denoted as  $\hat{\mathbf{x}}_0$ , and we assume that this estimate is a sufficient statistic for  $\mathbf{x}_\tau$ . This results in a first assumption  $p(\mathbf{y}|\mathbf{x}_\tau, \mathbf{h}) \approx p(\mathbf{y}|\hat{\mathbf{x}}_0, \mathbf{h})$ . The estimate  $\hat{\mathbf{x}}_0(\mathbf{x}_\tau)$  is obtained as the posterior mean of  $\mathbf{x}_0$  knowing  $\mathbf{x}_\tau$  and is derived using Tweedie's formula, i.e. one-step denoising of  $\mathbf{x}_\tau$ :

$$\hat{\mathbf{x}}_0(\mathbf{x}_\tau) \triangleq \mathbb{E}[\mathbf{x}_0|\mathbf{x}_\tau] \approx \mathbf{x}_\tau - \sigma^2(\tau) \mathbf{s}_\theta(\mathbf{x}_\tau, \tau). \quad (6)$$

In order to approximate  $p(\mathbf{y}|\hat{\mathbf{x}}_0, \mathbf{h})$ , previous work [26] models the error between  $\mathbf{y}$  and  $\mathbf{h} * \hat{\mathbf{x}}_0$  to follow a zero-mean Gaussian distribution in the time domain. The corresponding expression for the likelihood score  $\nabla_{\mathbf{x}_\tau} \log p(\mathbf{y}|\mathbf{x}_\tau, \mathbf{h})$  is then a simple weighted  $L^2$ -distance between  $\mathbf{y}$  and  $\mathbf{h} * \hat{\mathbf{x}}_0$ . However we observed that far better dereverberation performance and speech quality can be achieved by substituting the obtained distance with a  $L^2$ -distance between compressed spectrograms instead. This is analogous to modelling the likelihood score as:

$$\nabla_{\mathbf{x}_\tau} \log p(\mathbf{y}|\mathbf{x}_\tau, \mathbf{h}) \approx -\zeta(\tau) \nabla_{\mathbf{x}_\tau} \mathcal{C}(\mathbf{y}, \mathbf{h} * \hat{\mathbf{x}}_0(\mathbf{x}_\tau)), \quad (7)$$

where  $\zeta(\tau)$  is a diffusion-time-dependent scaling parameter that controls the influence of the likelihood score term in the sampling trajectory, and  $\mathcal{C}(\cdot, \cdot)$  is the following cost function:

$$\mathcal{C}(\mathbf{u}, \mathbf{v}) = \frac{1}{M} \sum_{m=1}^M \sum_{k=1}^K \|S_{\text{comp}}(\mathbf{u})_{m,k} - S_{\text{comp}}(\mathbf{v})_{m,k}\|_2^2. \quad (8)$$

There,  $S_{\text{comp}}(\mathbf{u}) = |\text{STFT}(\mathbf{u})|^{2/3} \exp\{j \angle \text{STFT}(\mathbf{u})\}$  is the magnitude-compressed spectrogram of  $\mathbf{u}$ . This cost function

**Algorithm 2** Inference algorithm

---

**Require:** Reverberant speech  $\mathbf{y}$

$\mathbf{x}_{\text{init}} \leftarrow \text{WPE}(\mathbf{y})$

Sample  $\mathbf{x}_N \sim \mathcal{N}(\mathbf{x}_{\text{init}}, \sigma_N^2 \mathbf{I})$  ▷ Warm initialization

Initialize  $\psi_N$  ▷ Initialize the RIR parameters

**for**  $n \leftarrow N, \dots, 1$  **do** ▷ Discrete step backwards

$\mathbf{s}_n \leftarrow \mathbf{s}_\theta(\mathbf{x}_n, \tau_n)$  ▷ Evaluate score model

$\hat{\mathbf{x}}_n \leftarrow \mathbf{x}_n - \sigma_n^2 \mathbf{s}_n$  ▷ Get one-step denoising estimate

$\hat{\mathbf{x}}_n \leftarrow \text{Rescale}(\hat{\mathbf{x}}_n)$  ▷ Constrain RMS power

$\psi_{n-1}^0 \leftarrow \psi_n$  ▷ Use RIR parameters from last step

**for**  $j \leftarrow 0, \dots, N_{\text{its}}$  **do** ▷ RIR optimization

$\mathcal{J}_{\text{RIR}}(\psi_{n-1}^j) \leftarrow \mathcal{C}(\mathbf{y}, \mathcal{A}_{\psi_{n-1}^j}(\hat{\mathbf{x}}_n)) + \mathcal{R}(\psi_{n-1}^j)$

$\psi_{n-1}^{j+1} \leftarrow \psi_{n-1}^j - \text{Adam}(\mathcal{J}_{\text{RIR}}(\psi_{n-1}^j))$  ▷ Opti. step

$\psi_{n-1}^{j+1} \leftarrow \text{clamp}(\psi_{n-1}^{j+1})$  ▷ Constrain Parameters

$\psi_{n-1} \leftarrow \psi_{n-1}^M$

$\mathbf{g}_n \leftarrow \zeta(\tau_n) \nabla_{\mathbf{x}_n} \mathcal{C}(\mathbf{y}, \mathcal{A}_{\psi_{n-1}}(\hat{\mathbf{x}}_n))$  ▷ LH score approx.

$\mathbf{x}_{n-1} \leftarrow \mathbf{x}_n - \sigma_n(\sigma_{n-1} - \sigma_n)(\mathbf{s}_n + \mathbf{g}_n)$  ▷ Update step

**return**  $\mathbf{x}_0$  ▷ Reconstructed audio signal

---

implies that we model the reconstruction error in the compressed STFT domain as a Gaussian with unknown variance  $\frac{1}{2\zeta(\tau)}$ . We apply this compression to boost low-energy components as typically observed in high frequencies of speech signals or in late reverberation tails, and account for the heavy-tailedness of speech distributions [4]. Such a strategy is also employed in [46] for data representation.

The parameter  $\zeta(\tau)$  balances a trade-off between adherence to the prior data distribution and fidelity to the observed data. We empirically resort to the same parameterization of  $\zeta(\tau)$  as in [32], [47]:

$$\zeta(\tau) = \frac{\sqrt{L} \tilde{\zeta}}{\|\nabla_{\mathbf{x}_\tau} \mathcal{C}(\mathbf{y}, \mathbf{h} * \hat{\mathbf{x}}_0(\mathbf{x}_\tau))\|_2}, \quad (9)$$

where  $\tilde{\zeta}$  is a fixed coefficient.

**IV. BLIND DIFFUSION-BASED DEREVERBERATION**

This section elaborates on the proposed method for blind dereverberation, where the impulse response  $\mathbf{h}$  is unknown. In Section IV-A, we define a reverberation operator  $\mathcal{A}_\psi(\cdot)$ , which comprises a structured parametric model of the RIR, with parameters  $\psi$ . This operator is summarized in Algorithm 1. The proposed inference method BUDDy, detailed in IV-B, performs joint speech dereverberation and RIR estimation by combining the conditional sampling from a diffusion model with an optimization of the RIR parameters. The complete inference procedure is summarized in Algorithm 2, and the processing pipeline is visualized in Fig. 2.

**A. Reverberation Operator**

1) *Subband Filtering:* In contrast to Section III, here we model reverberation using a subband filtering approximation in the short-time Fourier transform (STFT) domain [48], [49]. Let  $\mathbf{H} := \text{STFT}(\mathbf{h}) \in \mathbb{C}^{N_h \times K}$  represent the STFT of a RIR  $\mathbf{h}$  with  $N_h$  time frames and  $K$  frequency bins. Similarly, let  $\mathbf{X} \in \mathbb{C}^{M \times K}$ , and  $\mathbf{Y}$ , denote the STFTs of anechoic  $\mathbf{x}_0$



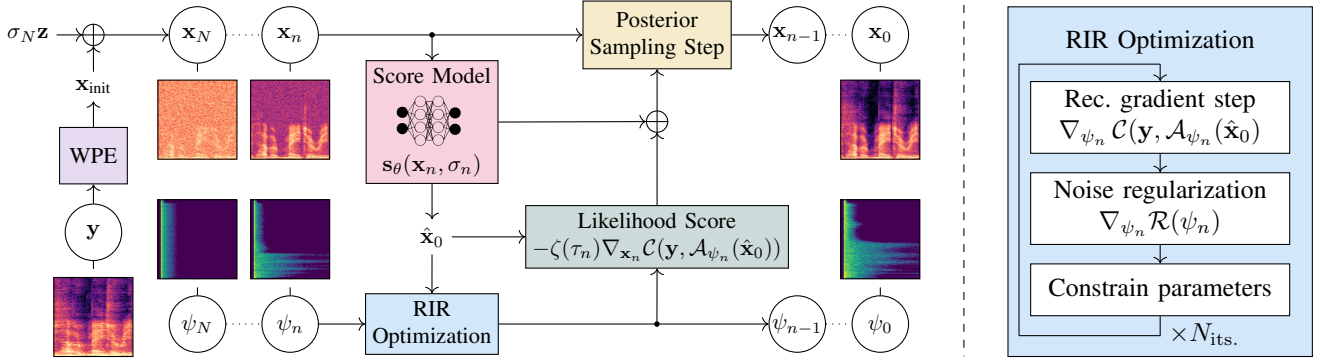


Fig. 2: BUDDy: joint optimization alternating between RIR estimation and posterior sampling for speech reconstruction [40].

and reverberant  $\mathbf{y}$  speech signals, respectively. The subband convolution operation applies independent convolutions along the time dimension of each frequency band:

$$\mathbf{Y}_{m,k} = \sum_{n=0}^{N_h} \mathbf{H}_{n,k} \mathbf{X}_{m-n,k}. \quad (10)$$

The resulting reverberant signal  $\mathbf{Y} \in \mathbb{C}^{(M+N_h-1) \times K}$  can be transformed to time domain by applying the inverse STFT. The subband filtering model only approximates the time-domain convolution, as it does not account for the spectral leakage between frequency bands. However, it is empirically found to be a valid assumption in many scenarios involving reverberation [7], [49], [50]. In our case, we noticed that adding 50% zero-padding to the end of the frames before computing the STFT was important to avoid cyclic convolution artifacts when retrieving the resulting signal to the time domain.

2) *Room Impulse Response Prior*: In the blind scenario, we need to estimate  $\mathbf{H}$ , which is an ill-posed problem task when not knowing the anechoic speech. Therefore, we need to constrain the space of possible solutions by imposing a prior on  $\mathbf{H}$ . We propose a structured, differentiable prior on  $\mathbf{H}$ , whose parameters  $\psi$  can be estimated through gradient descent. We denote the complete forward reverberation operator, including forward and inverse STFT operations, as  $\mathcal{A}_\psi(\cdot) : \mathbb{R}^L \rightarrow \mathbb{R}^{L+L_h-1}$ . The whole processing pipeline is summarized in Algorithm 1 with each component detailed below.

We denote as  $\mathbf{A} \in \mathbb{R}^{N_h \times K}$  and  $\Phi \in \mathbb{R}^{N_h \times K}$  the RIR magnitudes and phases, respectively. Following [11], we adopt an exponential decay model with learnable parameters controlling the decay time. Since room materials exhibit frequency-dependent absorption behavior, we parameterize the magnitude matrix  $\mathbf{A}$  as a multi-band exponential decay model defined in  $B < K$  frequency bands. Let  $\mathbf{A}' \in \mathbb{R}^{N_h \times B}$  be the subsampled version of  $\mathbf{A}$  in the  $B$  selected frequency bands. Each frequency band  $b$  is characterized by its weight  $w_b$  and exponential decay rate  $\alpha_b$ , such that the corresponding subband magnitude filter is derived as

$$\mathbf{A}'_{n,b} = w_b \cdot e^{-\alpha_b n}. \quad (11)$$

Note that our parameterization can be extended to model coupled spaces by employing several decay parameters per

band and summing their respective contributions [51]. We found it beneficial to constrain  $w_b$  and  $\alpha_b$  within a limited range to stabilize the optimization, specially at early stages. This is achieved by clamping the parameters to predefined minimum and maximum values after every optimization iteration, as specified in Appendix C1c. Once the parameters are estimated, we reconstruct the  $K$ -bands magnitudes  $\mathbf{A}$  by interpolating the subsampled  $\mathbf{A}'$  as  $\mathbf{A} = \exp(\text{lerp}(\log(\mathbf{A}')))$ , where  $\text{lerp}$  represents linear interpolation on the frequency scale. For this purpose, we employ the `torchcde` library, which facilitates efficient and differentiable interpolation [52]. After interpolation of the magnitude matrix, we then obtain the time-frequency RIR  $\mathbf{H}$  by multiplying the magnitude matrix  $\mathbf{A}$  with the complex phase exponentials:

$$\mathbf{H} = \mathbf{A} \odot e^{j\Phi}, \quad (12)$$

where  $j$  is the imaginary number and  $\odot$  represents element-wise multiplication. Given the general lack of phase structure, we optimize each phase factor in  $\Phi$  independently. The RIR model  $\psi = \{\Phi, (w_b, \alpha_b)_{b=1, \dots, B}\}$  ultimately contains  $2 \times B + N_h \times K$  optimizable parameters.

3) *Projections*: We extend our forward reverberation operator with a series of projections to increase the likelihood of generating plausible RIRs. Thus, the time-frequency RIR  $\mathbf{H}$  is further processed as:

$$\bar{\mathbf{H}} = \text{STFT}(\delta \oplus \mathcal{P}_{\min}(\text{iSTFT}(\mathbf{H}))). \quad (13)$$

This primarily ensures STFT consistency of  $\bar{\mathbf{H}}$ , exploiting the redundancy of the STFT representation and imposing inter-frame correlations between the RIR phases  $\Phi$ . We then enforce that the time-domain RIR estimate  $\mathbf{h}$  has minimum-phase lag, using the Hilbert transform-based method in [53]. This is indicated by the operator  $\mathcal{P}_{\min}$  and guarantees stability of the inverse RIR filter [2]. We refer the reader to Appendix A for further details. Finally, the operation  $\delta \oplus (\cdot)$  replaces the first sample of the time-domain RIR with a unit impulse. This has the effect of injecting knowledge of the direct path in  $\bar{\mathbf{H}}$ , and further requires us to correct the magnitude matrix  $\mathbf{A}$  to account for this operation. It is important to note that these steps are integral to the reverberation operator  $\mathcal{A}_\psi(\cdot)$ , which maps the parameters  $\psi$  to the convolved signal  $\mathcal{A}_\psi(\hat{\mathbf{x}}_0)$ , as outlined in Algorithm 1. Since all operations are differentiable, we compute gradients with respect to  $\psi$  by backpropagating

through all operations. We propose a detailed ablation study of these projection and correction steps in Section V-A6.

### B. Blind Dereverberation Inference

We aim to solve the following joint dereverberation and RIR parameter optimization problem:

$$\hat{\mathbf{x}}_0, \hat{\psi} = \arg \min_{\mathbf{x}_0, \psi} \mathcal{C}(\mathbf{y}, \mathcal{A}_\psi(\mathbf{x}_0)) + \mathcal{R}(\psi) \quad \text{s.t. } \mathbf{x}_0 \sim p_{\text{data}} \quad (14)$$

where  $\mathcal{C}(\mathbf{y}, \mathcal{A}_\psi(\mathbf{x}_0))$  is the reconstruction error with  $\mathcal{C}$  the cost function introduced in (8), and  $\mathcal{R}(\psi)$  is a RIR regularization term. This objective seeks to find the optimal speech  $\hat{\mathbf{x}}_0$  and RIR parameters  $\hat{\psi}$  that minimize both losses while imposing the soft constraint that the estimated signal  $\hat{\mathbf{x}}_0$  should adhere to the anechoic speech distribution  $p_{\text{data}}$ . We leverage the pre-trained score model  $s_\theta(\mathbf{x}_\tau, \tau)$  trained on anechoic speech to enforce this constraint.

We optimize (14) by solving the following ODE, obtained from the classical probability-flow ODE (1) where we injected the specified diffusion parameters of Karras et al. [44] and the likelihood score approximation derived in (7):

$$d\mathbf{x}_\tau = -\tau [s_\theta(\mathbf{x}_\tau, \tau) - \zeta(\tau) \nabla_{\mathbf{x}_\tau} \mathcal{C}(\mathbf{y}, \mathcal{A}_{\psi_\tau}(\hat{\mathbf{x}}_0))] d\tau. \quad (15)$$

The regularization term  $\mathcal{R}(\psi)$  introduced in (14) is:

$$\mathcal{R}(\psi) = \frac{1}{N_h} \sum_{m=1}^{N_h} \sum_{k=1}^K \|S_{\text{comp}}(\hat{\mathbf{h}}_\psi)_{m,k} - S_{\text{comp}}(\hat{\mathbf{h}}_{\psi'} + \sigma' \mathbf{v})_{m,k}\|_2^2, \quad (16)$$

where  $\hat{\mathbf{h}}_\psi = \mathcal{A}_\psi(\delta)$  is the current time-domain RIR estimate and  $\mathbf{v} \sim \mathcal{N}(\mathbf{0}, \mathbf{I})$  is a vector of white Gaussian noise. The noise level schedule  $\sigma'(\tau)$  is similar to the score model schedule  $\sigma(\tau)$  but its values are limited to avoid having too much noise at early steps (see Appendix C1a). The term  $\hat{\mathbf{h}}_{\psi'}$  represents a copy of  $\hat{\mathbf{h}}_\psi$ , such that the arg min in (14) does not apply to it. In other terms, we detach the gradients of  $\hat{\mathbf{h}}_\psi$  from the optimization graph to obtain  $\hat{\mathbf{h}}_{\psi'}$ , similar to what is done in e.g. [54] for guiding data reconstruction. We provide in Appendix B a short analysis of the regularization objective  $\mathcal{R}(\psi)$ . We show that this term injects multiplicative noise with standard deviation  $\sigma'(\tau)$  in the RIR parameter gradients, which arguably smoothes the RIR parameter search.

During optimization, we further rescale the denoised speech estimate  $\hat{\mathbf{x}}_0$  so that its root-mean-square power (RMS) matches the average RMS power of clean speech computed on the training set. Using this additional constraint helps lifting the indeterminacy when jointly optimizing the speech  $\mathbf{x}_0$  and RIR parameters  $\psi$ . This step is included in our ablation study in Section V-A6.

In order to guide and accelerate reverse diffusion, it is often beneficial to use warm initialization, i.e. to let the reverse diffusion process start from a speech sample  $\mathbf{x}_T \sim \mathcal{N}(\mathbf{x}_{\text{init}}, \sigma^2(T)\mathbf{I})$ , where  $\mathbf{x}_{\text{init}}$  has some interesting cues about the clean signal we wish to estimate. Similar to [34], we obtain the initial mean signal  $\mathbf{x}_{\text{init}}$  through WPE [7], a blind dereverberation algorithm based on variance-normalized delayed linear prediction. WPE performs mild dereverberation, which allows us to get closer to the clean speech, while not

introducing too many distortions to the signal. As WPE is blind and unsupervised, our method remains fully blind and unsupervised as well.

## V. EXPERIMENTS AND RESULTS

In this section, we provide a comprehensive evaluation of BUDDy across various datasets and experimental setups. We detail the methodologies and baselines employed and present the results of our experiments.

### A. Speech Dereverberation

We present dereverberation results on 16kHz speech data, building upon the experiments conducted in prior work [40].

1) *Data*: We use VCTK [57] as clean speech, selecting 103 speakers for training, 2 for validation and 2 for testing. The total dataset represents 44h of audio, which we down-sample to 16kHz for our experiments. We curate RIRs from various public datasets [58]–[66]. In total we approximately obtain 10k RIRs, and split them between training, validation and testing using ratios 0.9/0.05/0.05. We also generate another RIR dataset for testing methods in a mismatched setting, using RIRs simulated with `pyroomacoustics` [67]. For ease of comparison, we choose simulation parameters such that the distributions of reverberation times and direct-to-reverberation ratios of the simulated mismatched dataset approximately match those of the real-recorded matched dataset.

2) *Baselines*: We compare our method BUDDy to several blind supervised baselines such as the predictive approach in [55], which will denote as PSE in the following (for *predictive speech enhancement*), and diffusion-based SGMSE+ [24] and StoRM [25]. The STFT-based diffusion model in SGMSE+ and StoRM uses supervision in both the network conditioning and the diffusion trajectory parameterization; PSE uses a classical  $L^2$ -distance between the clean target and its estimate and has virtually the same architecture as SGMSE+. These methods require coupled reverberant/anechoic speech, which we generate using our curated RIR and anechoic speech datasets. The reverberant speech is obtained by first aligning the direct path of the RIR to its first sample, then convolving the anechoic speech from VCTK with the resulting RIR, and finally normalizing it to reach the same loudness [68] as the anechoic speech.

We also include blind unsupervised approaches leveraging traditional methods such as WPE [7] and Yohena and Yatabe [8], as well as generative models Saito et al. [34], GibbsDDRM [35] and RVAE-EM [38]. Please see Appendix C1b for more details on baselines.

3) *Hyperparameters*: As in [26], [40], we implement the unconditional score model architecture with NCSN++M [25], [55], which is a convolution-based neural network operating in the complex STFT domain. NCSN++M is also used as the base architecture for PSE, SGMSE+ and StoRM. Details on the architecture, training configuration, reverberation operator and diffusion hyperparameters can be found in appendices C1a., C1c and C1d, respectively.

TABLE II: *Speech dereverberation results on reverberant VCTK datasets. We indicate for each method in the table whether it is supervised or not. Boldface numbers indicate best performance for supervised and unsupervised methods separately.*

Method	Unsup.	Matched			Mismatched		
		DNS-MOS	PESQ	ESTOI	DNS-MOS	PESQ	ESTOI
Reverberant	-	3.14 ± 0.52	1.61 ± 0.37	0.50 ± 0.14	3.05 ± 0.47	1.57 ± 0.29	0.47 ± 0.11
PSE	✗	3.75 ± 0.38	2.85 ± 0.55	0.80 ± 0.10	3.61 ± 0.39	2.08 ± 0.47	0.64 ± 0.09
SGMSE+M [24], [55]	✗	3.88 ± 0.32	2.99 ± 0.48	0.78 ± 0.09	3.74 ± 0.34	2.48 ± 0.47	<b>0.69 ± 0.09</b>
StoRM [25]	✗	<b>3.90 ± 0.33</b>	<b>3.33 ± 0.48</b>	<b>0.82 ± 0.10</b>	<b>3.83 ± 0.32</b>	<b>2.51 ± 0.53</b>	0.67 ± 0.09
Yohena and Yatabe [8]	✓	2.99 ± 0.56	1.80 ± 0.33	0.55 ± 0.12	2.94 ± 0.44	1.71 ± 0.29	0.51 ± 0.10
WPE [56]	✓	3.24 ± 0.54	1.81 ± 0.42	0.57 ± 0.14	3.10 ± 0.48	1.74 ± 0.37	0.54 ± 0.12
Saito et al. [34]	✓	3.22 ± 0.56	1.68 ± 0.40	0.51 ± 0.13	3.12 ± 0.52	1.70 ± 0.33	0.52 ± 0.10
GibbsDDRM [35]	✓	3.33 ± 0.53	1.70 ± 0.37	0.51 ± 0.13	3.30 ± 0.52	1.75 ± 0.36	0.52 ± 0.11
RVAE-EM [38]	✓	3.05 ± 0.53	1.83 ± 0.32	0.54 ± 0.11	3.00 ± 0.45	1.76 ± 0.30	0.52 ± 0.10
BUDDy (ours)	✓	<b>3.76 ± 0.41</b>	<b>2.30 ± 0.53</b>	<b>0.66 ± 0.12</b>	<b>3.74 ± 0.38</b>	<b>2.24 ± 0.54</b>	<b>0.65 ± 0.12</b>

4) *Instrumental metrics*: For instrumental evaluation of the speech dereverberation performance, we use the intrusive Perceptual Evaluation of Speech Quality (PESQ) [69] and extended short-term objective intelligibility (ESTOI) [70] for assessment of speech quality and intelligibility respectively. We also use the non-intrusive DNS-MOS [71], a DNN-based mean opinion score (MOS) approximation following the ITU-T P.835 recommendation [72].

5) *Instrumental evaluation results*: We display in Table II the dereverberation results for all blind methods, both supervised and unsupervised. Blind supervised approaches-PSE, SGMSE+ and StoRM generally perform better than unsupervised methods as they benefit from supervision at training time. However, we can observe the limited generalization ability of supervised approaches in the setting where acoustic conditions are mismatched, i.e. when using simulated RIRs. Our method BUDDy, however, seamlessly adapts to changing acoustics since it was trained without supervision. This enables BUDDy to keep the same performance on both *matched* and *mismatched* datasets, where supervised methods like PSE lose as much as 0.77 PESQ points in mismatched conditions. Furthermore, BUDDy performs far better than all other blind unsupervised baselines. For instance, BUDDy outperforms WPE by as much as 0.50 PESQ and 0.10 ESTOI points. Indeed, traditional unsupervised methods [7], [8] only draw limited benefits from their uninformed Gaussian prior on anechoic speech, while diffusion-based Saito et al. [34] and GibbsDDRM [35] seem to only marginally deviate from their WPE initialization. RVAE-EM [38] also obtains low instrumental scores, but informal listening suggested that its dereverberation abilities were superior to those of WPE.

6) *Ablation study*: We conduct an ablation study to evaluate the impact of the projection step (13) introduced in the operator optimization (see Section IV-A). We present the results in Table III and observe that, although the minimum-phase consistency projection has a theoretical justification as a mean to enhance the stability of the inverse RIR during optimization, its practical effect appears negligible. However, we observe that the other operations in the projection step,

i.e. STFT consistency, enforcement of the direct path, and speech magnitude constraint, are all instrumental in guiding BUDDy toward a solution with higher fidelity to clean speech, as measured by PESQ. We show DNS-MOS figures out of completeness. However, DNS-MOS variations are small across ablations and not indicative of fidelity to reference speech as DNS-MOS is not an intrusive metric.

Additionally, we examine the effect of parameterizing the likelihood model with a  $L^2$ -distance on compressed spectrograms rather than on waveforms as in previous work [26]. To do so, we replace the cost function  $C(\cdot, \cdot)$  from (8), which is based on compressed spectrograms, with a simpler waveform-domain  $L^2$ -distance. The results clearly show the superiority of using a cost function on compressed spectrograms.

7) *Listening experiment*: Instrumental metrics offer only limited insights into the performance of dereverberation algorithms [73]. We therefore conduct a listening experiment based on the MUSHRA recommendation [74] to assess the performance of BUDDy as perceived by human listeners. The test comprised 12 pages, featuring 6 reverberant speech utterances from each of the *matched* and *mismatched* datasets. Participants were asked to rate the different stimuli with a single number representing overall quality, taking into account factors such as voice distortion, residual reverberation, and potential artifacts [73]. The test stimuli include our proposed method BUDDy, the unsupervised WPE [7] and RVAE-EM [38], as well as the supervised baselines PSE and SGMSE+ [24]. Further details on the organization of the listening experiment are reported in Appendix C1e.

The results of the experiment are presented in Fig. 3. It can be observed that the unsupervised baselines WPE and RVAE-EM received low scores. Yet, RVAE-EM performs consistently better than WPE in this listening experiment, as opposed to what is suggested by instrumental metrics in Table II. In the matched test set (Fig. 3a), BUDDy obtained significantly lower scores than PSE and SGMSE+ ( $p < 0.001$  in a paired Welch test). However, in the mismatched set, PSE and SGMSE+ suffered a decrease in performance, losing up to 20 points (out of 100), while BUDDy maintained similar scores. In that case, there is no significant difference in performance between

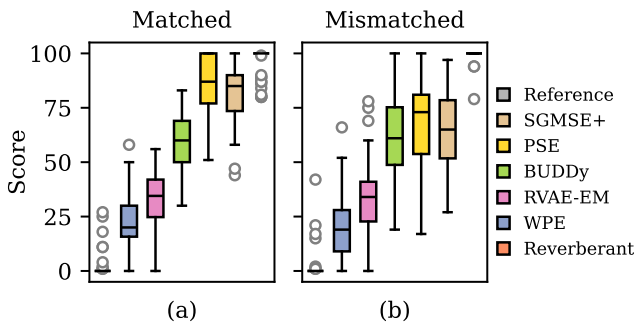


Fig. 3: Listening test results on reverberant VCTK datasets. The boxplot shows first quartile, median and third quartile.

the three approaches ( $p > 0.1$ ), which closes the gap between BUDDy and the top-performing supervised baselines in this mismatched setting, highlighting the advantage provided by unsupervised learning.

### B. Singing Voice Dereverberation

We extend our evaluation benchmark to include the related task of singing voice dereverberation.

1) *Data*: We collect several publicly available singing voice datasets [75]–[80]. These datasets feature over 94 h of studio-quality solo singing from a diverse array of singers and singing styles, spanning various languages. The majority of the recordings are in Chinese, followed by English, Japanese, and Korean. All datasets are down-sampled to 44.1 kHz. For testing, similar to [35], we use the sung part of NHSS [81], [82]. The NHSS dataset contains 100 English-language pop songs, 10 for each of the five male and five female singers recruited. We select a subset (90%) of the RIRs curated for the VCTK-based experiments, such that we only retain the RIRs whose original sample rate is at least 44.1kHz.

2) *Baselines*: We evaluate the performance of BUDDy against two unsupervised baselines: WPE [7] and the unsupervised method from Saito et al. [34] which was originally designed for singing voice dereverberation. Due to the lack of established supervised baselines for this specific task, we created our own by adapting the diffusion model from BUDDy to a supervised setting. In this adaptation, we trained a diffusion model on dry singing voice using the same architecture and hyperparameters as the unconditional model in BUDDy,

TABLE III: Ablation study on reverberant VCTK dataset.

Method	PESQ	DNS-MOS
Reverberant	$1.61 \pm 0.37$	$3.14 \pm 0.52$
BUDDy	<b><math>2.30 \pm 0.53</math></b>	$3.76 \pm 0.41$
- Minimum-phase Consistency	<b><math>2.30 \pm 0.57</math></b>	$3.81 \pm 0.40$
- RMS Power Constraint	$2.22 \pm 0.50$	$3.64 \pm 0.50$
- Fixed Direct Path	$2.10 \pm 0.46$	$3.78 \pm 0.44$
- STFT Consistency	$1.96 \pm 0.41$	<b><math>3.84 \pm 0.39</math></b>
$L^2$ -Distance for $\mathcal{C}(\cdot, \cdot)$	$1.86 \pm 0.47$	$3.36 \pm 0.56$

TABLE IV: Singing voice dereverberation results on reverberant NHSS dataset. We indicate each method whether it is unsupervised or not.

Method	Unsup.	$\ell^1$ STFT	FAD (VGGish)
Reverberant	-	$1.98 \pm 0.66$	6.41
Conditional Diffusion	✗	<b><math>1.56 \pm 0.48</math></b>	1.71
WPE [7]	✓	$2.02 \pm 0.65$	4.53
Saito et al. [34]	✓	$1.95 \pm 0.65$	5.41
BUDDy (ours)	✓	$1.92 \pm 0.60$	<b>1.32</b>

but added a paired sample of reverberant voice as a condition. The conditioning sample is incorporated into the architecture by stacking it in the channel dimension. This setup resembles the “variance exploding” approach used by Gonzalez et al. for speech enhancement [83]. We train all methods on our singing voice dataset detailed in the previous section.

3) *Hyperparameters*: As in [32] for music restoration, we use the UNet architecture proposed in [84] without self-attention blocks, and wrap the computations within an invertible Constant-Q Transform (CQT) [85]. The CQT produces a time-frequency representation where pitch transpositions are equivalent to frequency-wise translations, highlighting its interest for processing signals with harmonic components such as singing voice and music. More details with regard to the architecture and specific training configuration and inference hyperparameters are reported in Appendix C2

4) *Evaluation metrics*: Objective metrics for evaluating singing voice restoration tasks are currently more limited compared to those available for speech processing. Following [34], we use the  $\ell^1$ -distance in the magnitude STFT domain and a Fréchet Audio Distance (FAD) using a VGGish embedding [86]. However, these are only limited in interpretability and hardly relate to listening impression [87], [88]. Therefore, we complete this evaluation benchmark with a listening test with 10 participants, using a similar setup as reported in Section V-A7. In this case, the test included 10 reverberant singing voice examples from the NHSS dataset, and the instructions were identical to those reported in Appendix C1e.

5) *Results*: The results from the instrumental evaluation are reported in Table IV and those from the listening test in Fig. 4. The results show that BUDDy largely outperforms the

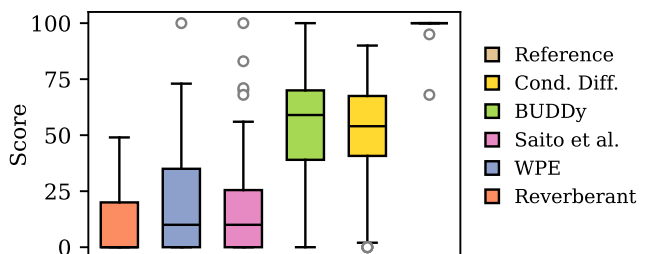


Fig. 4: Listening test results on singing voice dataset. The boxplot shows first quartile, median and third quartile.



unsupervised baselines and is on-par with the conditional diffusion model that benefited from supervision at training time. We found no statistically significant difference between the listening test scores of BUDDy and the conditional diffusion model (p-value of 0.55 in a paired Welch test).

### C. Room Impulse Response Estimation

BUDDy is not only designed as a dereverberation algorithm but also functions as a blind unsupervised RIR estimator. We evaluate its performance for RIR estimation using the same speech model and data we employed for speech dereverberation in Section V-A.

1) *Baseline:* We benchmark BUDDy against FiNS [41], a deep neural network (DNN)-based approach trained to estimate time-domain RIRs directly from reverberant speech. FiNS comprises a 1D-convolutional encoder and a two-component decoder. The first decoder component estimates the late tail of the RIR by passing noise signals through a trainable filterbank containing several FIR filters. The second decoder component directly estimates the direct path and early reflections in the time-domain. In contrast to BUDDy, FiNS relies on supervised learning, thus requiring a paired dataset of reverberant speech and RIRs. We use an unofficial re-implementation<sup>2</sup> and train the model on our VCTK-based reverberant speech dataset.

2) *Evaluation metrics:* Due to the highly ill-posed nature of the blind RIR estimation problem and the statistical nature of late reflections [11], we refrain from using element-wise distances, such as error-to-signal ratios, to evaluate the performance of RIR estimators. Instead, it is arguably more important to preserve the acoustic and perceptual properties of the reference RIR [89]. On the other hand, single metrics such as the  $T_{60}$  reverberation time or clarity index  $C_{50}$  do not

account for frequency-specific estimation errors. We therefore employ a subband reverberation time  $T_{60}$  and clarity index  $C_{50}$ , with subbands spanning octaves. This enables to keep a high-level representation of the acoustical properties while allowing enough granularity on the spectral attributes of the RIR. The reverberation time  $T_{60}$  is defined for a diffuse sound field as the time it takes for its energy decay curve (EDC) to decay by 60dB [1]. To compute  $T_{60}$  from a RIR while avoiding the effects of the noise floor, we first determine  $T_{30}$  and extrapolate it to  $T_{60}$  by multiplying by a factor of 2. We calculate  $T_{30}$  as the time required for the EDC to decrease from -5 dB to -35 dB relative to the initial level to eliminate the influence of the direct path. This measure is computed in each octave band separately. The octave clarity index  $C_{50}$  is the ratio (in dB) between the energy in the 50 first milliseconds and the energy in the remaining of the RIR, calculated in the corresponding octave band [1]. Consequently, we compute the absolute error between the  $T_{60}$  and  $C_{50}$  values calculated for each octave from the estimated RIR and those from the ground truth RIR.

3) *Results:* The results for both matched and mismatched test sets are plotted in Fig. 5. In the matched condition, FiNS and BUDDy achieve similar  $T_{60}$  error rates at low- and mid-range frequency bands, while BUDDy’s performance decreases at high frequencies (Fig. 5a). Our intuition is that the lower RIR estimation abilities of BUDDy at high frequencies can be linked to the tendency of diffusion models to generate high-frequency components at the later stages of the reverse diffusion process [90]. Consequently, there is less information available for optimizing the RIR parameters in this range, negatively affecting parameter convergence. A similar trend is observed for the  $C_{50}$  error (Fig. 5c). Furthermore, BUDDy generally achieves lower  $C_{50}$  error than FiNS in the mid-frequency range, where most of the speech content lies.

In the mismatched setting, FiNS struggles to generalize

<sup>2</sup><https://github.com/kyungyunlee/fins>

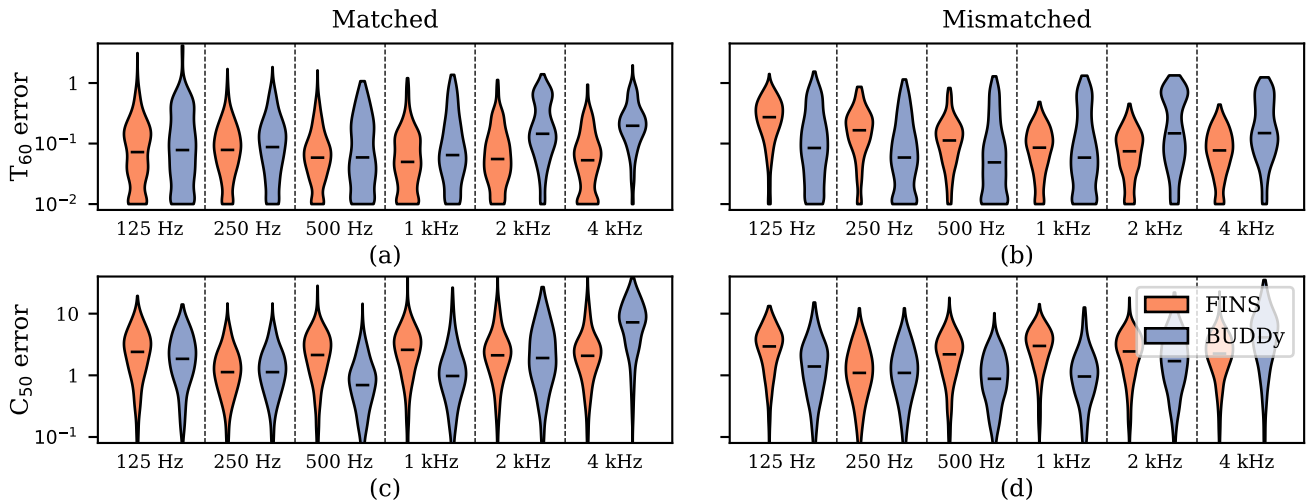


Fig. 5: RIR estimation metrics calculated for each octave on the reverberant VCTK dataset. The violin plots show the results distribution, with the median highlighted. Lower values indicate better performance. FiNS [41] is trained in a supervision fashion whereas BUDDy is unsupervised.

because of its supervised training setup. As a result, BUDDY outperforms FiNS in both  $T_{60}$  and  $C_{50}$  error at low and mid-frequency bands (Figs. 5b) and 5d). At higher frequencies, BUDDY's  $T_{60}$  estimation performance still remains slightly inferior to FiNS, though the gap is noticeably smaller than in the matched setting. Regarding  $C_{50}$ , BUDDY outperforms FiNS on all frequency domains but the higher, 4-kHz-centered band. This increased relative performance of BUDDY compared to FiNS highlights the benefits of leveraging unsupervised training for RIR estimation in variable acoustic conditions.

## VI. CONCLUSION

In this paper, we presented an unsupervised method that simultaneously performs blind dereverberation and RIR estimation using diffusion models. Our results highlight the importance of joint speech and RIR estimation in contrast to plugging estimated RIRs into informed dereverberation methods. The proposed method, BUDDY, yields state-of-the-art performance among unsupervised approaches for blind speech and singing voice dereverberation, outperforming both traditional and diffusion-based methods. Unlike blind supervised methods, which often struggle with generalization to unseen acoustic conditions, our unsupervised approach naturally overcomes this limitation due to its ability to adapt the reverberation operator to a broad range of room impulse responses. This holds as well for RIR estimation, as we show that the RIR estimation performance of BUDDY surpasses that of a state-of-the-art supervised DNN-based technique in mismatched acoustic conditions while being on par in a matched setting.

## ACKNOWLEDGEMENTS

We would like to thank Koichi Saito, Fumikuri Yohena and Kohei Yatabe for providing us with code and guidance through their methods.

## REFERENCES

- [1] P. A. Naylor and N. D. Gaubitch, *Speech Dereverberation*, vol. 59, Springer, 2011.
- [2] M. Miyoshi and Y. Kaneda, "Inverse filtering of room acoustics," *IEEE TASLP*, vol. 36, no. 2, pp. 145–152, 1988.
- [3] T. Gerkmann and E. Vincent, "Spectral masking and filtering," in *Audio Source Separation and Speech Enhancement*, E. Vincent, T. Virtanen, and S. Gannot, Eds. John Wiley & Sons, 2018.
- [4] T. Gerkmann and R. Martin, "Empirical distributions of DFT-domain speech coefficients based on estimated speech variances," in *Proc. IWAENC*, 2010.
- [5] I. Kodrasi, T. Gerkmann, and S. Doclo, "Frequency-domain single-channel inverse filtering for speech dereverberation: Theory and practice," in *Proc. Int. Conf. Acoust. Speech Signal Process.*, 2014.
- [6] J. Mourjopoulos, P. Clarkson, and J. Hammond, "A comparative study of least-squares and homomorphic techniques for the inversion of mixed phase signals," in *Proc. Int. Conf. Acoust. Speech Signal Process.*, 1982.
- [7] T. Nakatani, B. Juang, T. Yoshioka, K. Kinoshita, M. Delcroix, and M. Miyoshi, "Speech dereverberation based on maximum-likelihood estimation with time-varying Gaussian source model," *IEEE TASLP*, vol. 16, no. 8, pp. 1512–1527, 2008.
- [8] F. Yohena and K. Yatabe, "Single-channel blind dereverberation based on rank-1 matrix lifting in time-frequency domain," in *Proc. Int. Conf. Acoust. Speech Signal Process.*, 2024.
- [9] D. Schmid, S. Malik, and G. Enzner, "A maximum a posteriori approach to multichannel speech dereverberation and denoising," in *Proc. IWAENC*, 2012.
- [10] A. Jukić, T. van Waterschoot, T. Gerkmann, and S. Doclo, "Speech dereverberation with convolutive transfer function approximation using map and variational deconvolution approaches," in *Proc. IWAENC*, 2014.
- [11] E. A. P. Habets, *Speech Dereverberation Using Statistical Reverberation Models*, pp. 57–93, Springer, London, 2010.
- [12] S. T. Neely and J. B. Allen, "Invertibility of a room impulse response," *J. Acoust. Soc. Am.*, vol. 66, no. 1, pp. 165–169, 1979.
- [13] T. Hikichi, M. Delcroix, and M. Miyoshi, "Inverse filtering for speech dereverberation less sensitive to noise and room transfer function fluctuations," *EURASIP J. Adv. Signal Process.*, 2007.
- [14] D. Wang and J. Chen, "Supervised speech separation based on deep learning: An overview," *IEEE TASLP*, vol. 26, no. 10, pp. 1702–1726, 2018.
- [15] D. S. Williamson and D. Wang, "Time-frequency masking in the complex domain for speech dereverberation and denoising," *IEEE/ACM TASLP*, vol. 25, no. 7, pp. 1492–1501, 2017.
- [16] K. Han, Y. Wang, D. Wang, W. S. Woods, I. Merks, and T. Zhang, "Learning spectral mapping for speech dereverberation and denoising," *IEEE/ACM TASLP*, vol. 23, no. 6, pp. 982–992, 2015.
- [17] X. Liu, S.-J. Chen, and J. H. Hansen, "Dual-path minimum-phase and all-pass decomposition network for single channel speech dereverberation," in *Proc. Int. Conf. Acoust. Speech Signal Process.*, 2024.
- [18] O. Ernst, S. E. Chazan, S. Gannot, and J. Goldberger, "Speech dereverberation using fully convolutional networks," in *Proc. EUSIPCO*, 2019.
- [19] Y. Zhao, D. Wang, B. Xu, and T. Zhang, "Monaural speech dereverberation using temporal convolutional networks with self attention," *IEEE/ACM TASLP*, vol. 28, pp. 1598–1607, 2020.
- [20] J.-M. Lemerrier, J. Richter, S. Welker, E. Moliner, V. Välimäki, and T. Gerkmann, "Diffusion models for audio restoration," *arXiv*, 2024.
- [21] J. Sohl-Dickstein, E. Weiss, N. Maheswaranathan, and S. Ganguli, "Deep unsupervised learning using nonequilibrium thermodynamics," in *Proc. ICML*, 2015.
- [22] J. Ho, A. Jain, and P. Abbeel, "Denoising diffusion probabilistic models," in *Proc. NeurIPS*, 2020.
- [23] Y. Song, J. Sohl-Dickstein, D. P. Kingma, A. Kumar, S. Ermon, and B. Poole, "Score-based generative modeling through stochastic differential equations," in *Proc. ICLR*, 2021.
- [24] J. Richter, S. Welker, J.-M. Lemerrier, B. Lay, and T. Gerkmann, "Speech enhancement and dereverberation with diffusion-based generative models," *IEEE/ACM TASLP*, vol. 31, pp. 2351–2364, 2023.
- [25] J.-M. Lemerrier, J. Richter, S. Welker, and T. Gerkmann, "StoRM: A diffusion-based stochastic regeneration model for speech enhancement and dereverberation," *IEEE TASLP*, vol. 31, pp. 2724–2737, 2023.
- [26] J.-M. Lemerrier, S. Welker, and T. Gerkmann, "Diffusion posterior sampling for informed single-channel dereverberation," in *Proc. WASPAA*, 2023.
- [27] H. Chung, J. Kim, M. T. Mccann, M. L. Klasky, and J. C. Ye, "Diffusion posterior sampling for general noisy inverse problems," in *Proc. ICLR*, 2023.
- [28] H. Chung, J. Kim, S. Kim, and J. C. Ye, "Parallel diffusion models of operator and image for blind inverse problems," in *Proc. CVPR*, 2023.
- [29] C. Laroche, A. Almansa, and E. Coupeté, "Fast diffusion em: a diffusion model for blind inverse problems with application to deconvolution," *IEEE/CVF WACV*, 2024.
- [30] Y. Sanghvi, Y. Chi, and S. H. Chan, "Kernel diffusion: An alternate approach to blind deconvolution," *arXiv*, 2023.
- [31] B. Nortier, M. Sadeghi, and R. Serizel, "Unsupervised speech enhancement with diffusion-based generative models," in *Proc. Int. Conf. Acoust. Speech Signal Process.*, 2024.
- [32] E. Moliner, F. Elvander, and V. Välimäki, "Blind audio bandwidth extension: A diffusion-based zero-shot approach," *arXiv*, 2024.
- [33] B. Kawar, M. Elad, S. Ermon, and J. Song, "Denoising diffusion restoration models," in *Proc. NeurIPS*, 2022.
- [34] K. Saito, N. Murata, T. Uesaka, C.-H. Lai, Y. Takida, T. Fukui, and Y. Mitsufuji, "Unsupervised vocal dereverberation with diffusion-based generative models," in *Proc. Int. Conf. Acoust. Speech Signal Process.*, 2023.
- [35] N. Murata, K. Saito, C.-H. Lai, Y. Takida, T. Uesaka, Y. Mitsufuji, and S. Ermon, "GibbsDDRM: A partially collapsed Gibbs sampler for solving blind inverse problems with denoising diffusion restoration," in *Proc. ICML*, 2023.
- [36] H. Attias, J. Platt, A. Acero, and L. Deng, "Speech denoising and dereverberation using probabilistic models," in *Proc. NeurIPS*, 2000.
- [37] D. Baby and H. Bourlard, "Speech dereverberation using variational autoencoders," in *Proc. Int. Conf. Acoust. Speech Signal Process.*, 2021.

- [38] P. Wang and X. Li, “RVAE-EM: Generative speech dereverberation based on recurrent variational auto-encoder and convolutive transfer function,” in *Proc. Int. Conf. Acoust. Speech Signal Process.*, 2024.
- [39] Z.-Q. Wang, “USDNet: Unsupervised speech dereverberation via neural forward filtering,” 2024.
- [40] E. Moliner, J.-M. Lemerrier, S. Welker, T. Gerkmann, and V. Välimäki, “BUDDy: Single-channel blind unsupervised dereverberation with diffusion models,” in *Proc. IWAENC*, 2024.
- [41] C. J. Steinmetz, V. K. Ithapu, and P. Calamia, “Filtered noise shaping for time domain room impulse response estimation from reverberant speech,” in *Proc. WASPAA*, 2021.
- [42] Y. Song and S. Ermon, “Generative modeling by estimating gradients of the data distribution,” in *Proc. NeurIPS*, 2019.
- [43] Z. Kong, W. Ping, J. Huang, K. Zhao, and B. Catanzaro, “DiffWave: A versatile diffusion model for audio synthesis,” *Proc. ICLR*, 2021.
- [44] T. Karras, M. Aittala, T. Aila, and S. Laine, “Elucidating the design space of diffusion-based generative models,” in *Proc. NeurIPS*, 2022.
- [45] P. Vincent, “A connection between score matching and denoising autoencoders,” *Neural Computation*, vol. 23, no. 7, pp. 1661–1674, 2011.
- [46] S. Welker, J. Richter, and T. Gerkmann, “Speech enhancement with score-based generative models in the complex STFT domain,” in *Proc. Interspeech*, 2022.
- [47] E. Moliner, J. Lehtinen, and V. Välimäki, “Solving audio inverse problems with a diffusion model,” in *Proc. Int. Conf. Acoust. Speech Signal Process.*, 2023.
- [48] M. M. Goodwin, “Realization of arbitrary filters in the stft domain,” in *Proc. WASPAA*, 2009.
- [49] Y. Avargel and I. Cohen, “System identification in the short-time fourier transform domain with crossband filtering,” *IEEE TASLP*, vol. 15, no. 4, pp. 1305–1319, 2007.
- [50] J.-M. Lemerrier, J. Tobergte, and T. Gerkmann, “Extending DNN-based multiplicative masking to deep subband filtering for improved dereverberation,” in *Proc. Interspeech*, 2023.
- [51] N. Xiang and P. M. Goggans, “Evaluation of decay times in coupled spaces: Bayesian data model selection,” *J. Acoust. Soc. Am.*, vol. 113, no. 5, pp. 2685–2697, 2003.
- [52] P. Kidger, J. Morrill, J. Foster, and T. Lyons, “Neural Controlled Differential Equations for Irregular Time Series,” *Proc. NeurIPS*, 2020.
- [53] A. V. Oppenheim and R. W. Schaffer, *Digital Signal Processing*, Prentice—Hall, 1975.
- [54] M. Mardani, J. Song, J. Kautz, and A. Vahdat, “A variational perspective on solving inverse problems with diffusion models,” in *Proc. ICLR*, 2024.
- [55] J.-M. Lemerrier, J. Richter, S. Welker, and T. Gerkmann, “Analysing discriminative versus diffusion generative models for speech restoration tasks,” in *Proc. Int. Conf. Acoust. Speech Signal Process.*, 2023.
- [56] T. Nakatani, T. Yoshioka, K. Kinoshita, M. Miyoshi, and B. Juang, “Blind speech dereverberation with multi-channel linear prediction based on short time fourier transform representation,” in *Proc. Int. Conf. Acoust. Speech Signal Process.*, 2008.
- [57] C. Valentini-Botinhao et al., “Reverberant speech database for training speech dereverberation algorithms and TTS models,” *University of Edinburgh*, 2016.
- [58] K. Prawda, S. J. Schlecht, and V. Välimäki, “Calibrating the Sabine and Eyring formulas,” *J. Acoust. Soc. Am.*, vol. 152, no. 2, pp. 1158–1169, 2022.
- [59] J. Eaton, N. D. Gaubitch, A. H. Moore, and P. A. Naylor, “The ACE challenge—Corpus description and performance evaluation,” in *Proc. WASPAA*, 2015.
- [60] M. Jeub, M. Schaefer, and P. Vary, “A binaural room impulse response database for the evaluation of dereverberation algorithms,” in *Proc. Int. Conf. Dig. Signal Process.*, 2009.
- [61] D. Fejgin, W. Middelberg, and S. Doclo, “Brudex database: Binaural room impulse responses with uniformly distributed external microphones,” in *Proc. ITG Conf. Speech Communication*, 2023.
- [62] U. of Kent, “Palimpsest impulse responses,” <https://research.kent.ac.uk/sonic-palimpsest/impulse-responses>.
- [63] G. Kearney et al., “Measuring the acoustical properties of the BBC Maida Vale recording studios for virtual reality,” *Acoustics*, vol. 4, no. 3, pp. 783–799, 2022.
- [64] B. U. of Technology, “BUT speech@FIT reverb database,” <https://speech.fit.vutbr.cz/software/but-speech-fit-reverb-database>.
- [65] T. Dietzen, R. A. Ali, M. Taseska, and T. van Waterschoot, “MYRIAD: A multi-array room acoustic database,” *EURASIP J. Audio Speech and Music Process.*, no. 17, pp. 1–14, 2023.
- [66] J. Traer and J. H. McDermott, “Statistics of natural reverberation enable perceptual separation of sound and space,” *National Academy of Sciences*, vol. 113, no. 48, pp. 7856–7865, 2016.
- [67] R. Scheibler, E. Bezzam, and I. Dokmanic, “Pyroomacoustics: A python package for audio room simulation and array processing algorithms,” in *Proc. Int. Conf. Acoust. Speech Signal Process.*, 2018.
- [68] G. International Telecommunication Union, “Algorithms to measure audio programme loudness and true-peak audio level,” Rec. BS.1770-4, Geneva, Switzerland, Oct. 20023.
- [69] A. Rix, J. Beerends, M. Hollier, and A. Hekstra, “Perceptual evaluation of speech quality (PESQ)-a new method for speech quality assessment of telephone networks and codecs,” in *Proc. Int. Conf. Acoust. Speech Signal Process.*, 2001.
- [70] J. Jensen and C. Taal, “An algorithm for predicting the intelligibility of speech masked by modulated noise maskers,” *IEEE/ACM TASLP*, vol. 24, no. 11, pp. 2009–2022, 2016.
- [71] C. K. A. Reddy, V. Gopal, and R. Cutler, “DNSMOS: A non-intrusive perceptual objective speech quality metric to evaluate noise suppressors,” *arXiv*, 2021.
- [72] G. International Telecommunication Union, “Subjective test methodology for evaluating speech communication systems that include noise suppression algorithm,” Rec. P.835, Geneva, Switzerland, Oct. 2003.
- [73] S. Goetze, A. Warzybok, I. Kodrasi, J. O. Jungmann, B. Cauchi, J. Rannies, E. A. P. Habets, A. Mertins, T. Gerkmann, S. Doclo, and B. Kollmeier, “A study on speech quality and speech intelligibility measures for quality assessment of single-channel dereverberation algorithms,” in *Proc. IWAENC*, 2014.
- [74] G. International Telecommunication Union, “Method for the subjective assessment of intermediate quality level of audio systems,” Rec. BS.1534-3, Geneva, Switzerland, Oct. 2015.
- [75] R. Huang et al., “Multi-singer: Fast multi-singer singing voice vocoder with a large-scale corpus,” in *ACM International Conference on Multimedia*, 2021.
- [76] Y. Wang et al., “Opencpop: A high-quality open source Chinese popular song corpus for singing voice synthesis,” *arXiv*, 2022.
- [77] L. Zhang et al., “M4singer: A multi-style, multi-singer and musical score provided Mandarin singing corpus,” in *Proc. NeurIPS*, 2022.
- [78] Z. Duan, H. Fang, B. Li, K. C. Sim, and Y. Wang, “The NUS sung and spoken lyrics corpus: A quantitative comparison of singing and speech,” in *Proc. APSIPA ASC*, 2013.
- [79] S. Choi, W. Kim, S. Park, S. Yong, and J. Nam, “Children’s song dataset for singing voice research,” in *Proc. ISMIR*, 2020.
- [80] J. Koguchi, S. Takamichi, and M. Morise, “PJS: Phoneme-balanced Japanese singing-voice corpus,” in *Proc. APSIPA ASC*, 2020.
- [81] B. Sharma, X. Gao, K. Vijayan, X. Tian, and H. Li, “NHSS: A speech and singing parallel database,” *arXiv*, 2020.
- [82] B. Sharma and H. Li, “A combination of model-based and feature-based strategy for speech-to-singing alignment,” in *Proc. Interspeech*, 2019.
- [83] P. Gonzalez, Z.-H. Tan, J. Østergaard, J. Jensen, T. S. Alstrøm, and T. May, “Investigating the design space of diffusion models for speech enhancement,” *arXiv*, 2023.
- [84] E. Moliner and V. Välimäki, “Diffusion-based audio inpainting,” *J. Audio Eng. Soc.*, vol. 72, pp. 100–113, Mar. 2024.
- [85] G. A. Velasco, N. Holighaus, M. Dörfler, and T. Grill, “Constructing an invertible constant-Q transform with non-stationary Gabor frames,” in *Proc. DAFX*, 2011.
- [86] K. Kilgour, M. Zuluaga, D. Roblek, and M. Sharifi, “Fréchet audio distance: A metric for evaluating music enhancement algorithms,” *arXiv preprint arXiv:1812.08466*, 2018.
- [87] N. Kandpal, O. Niteo, and Z. Jin, “Music enhancement via image translation and vocoding,” in *Proc. Int. Conf. Acoust. Speech Signal Process.*, 2022.
- [88] A. Gui, H. Gamper, S. Braun, and D. Emmanouilidou, “Adapting Fréchet audio distance for generative music evaluation,” in *Proc. Int. Conf. Acoust. Speech Signal Process.*, 2024, pp. 1331–1335.
- [89] G. D. Santo, K. Prawda, S. J. Schlecht, and V. Välimäki, “Similarity metrics for late reverberation,” in *Proc. Asilomar Conf. Signal Sys. Comp.*, 2024.
- [90] X. Yang, D. Zhou, J. Feng, and X. Wang, “Diffusion probabilistic model made slim,” in *Proc. CVPR*, 2023.
- [91] D. P. Kingma and J. Ba, “Adam: A method for stochastic optimization,” *Proc. ICLR*, 2015.

## APPENDIX

## A. Minimum phase constraint

The minimum-phase constraint in Section IV-A takes the time-domain RIR  $\mathbf{h}$  and computes the minimum-delay phase  $\Theta$  as:

$$\Theta = -\text{Im}[\mathcal{H}(\log|\mathcal{F}(\mathbf{h})|)], \quad (17)$$

where  $\mathcal{F}$  is the Fourier transform and  $\mathcal{H}$  the Hilbert transform:

$$\mathcal{H}(\mathbf{x}) \triangleq \mathcal{F}^{-1}(-j \cdot \text{sign}(\omega)\mathcal{F}(\mathbf{x})) \quad (18)$$

The minimum-delay corrected time-domain RIR is then obtained by replacing the original phase with the obtained minimum-delay phase:

$$\mathbf{h}_{\min} = \mathcal{F}^{-1}(|\mathcal{F}(\mathbf{h})|e^{j\Theta}) \quad (19)$$

It is worth noting that all the operations involved in this method are differentiable, which allows backpropagation throughout the process.

## B. Noise regularization

We introduce in Section IV-B a noise regularization term, which we can write in a simplified fashion, ignoring the sums and indexations, as:

$$\mathcal{R}(\psi) = \|S_{\text{comp}}(\hat{\mathbf{h}}_{\psi}) - S_{\text{comp}}(\hat{\mathbf{h}}_{\psi'} + \sigma'\mathbf{v})\|_2^2, \quad (20)$$

The gradient computed during optimization is obtained as:

$$\begin{aligned} \frac{\partial \mathcal{R}(\psi)}{\partial \psi} &= 2 \left( S_{\text{comp}}(\hat{\mathbf{h}}_{\psi}) - S_{\text{comp}}(\hat{\mathbf{h}}_{\psi'} + \sigma'\mathbf{v}) \right) \\ &\quad \times \frac{\partial S_{\text{comp}}}{\partial \hat{\mathbf{h}}_{\psi}} \times \left( \frac{\partial \hat{\mathbf{h}}_{\psi}}{\partial \psi} - \underbrace{\frac{\partial \hat{\mathbf{h}}_{\psi'}}{\partial \psi}}_0 \right) \\ &\approx -2\sigma'\mathbf{v} \left[ \frac{\partial S_{\text{comp}}}{\partial \hat{\mathbf{h}}_{\psi}} \right]^2 \frac{\partial \hat{\mathbf{h}}_{\psi}}{\partial \psi} \end{aligned}$$

where we have ignored second- and higher-order Taylor expansion terms of  $S_{\text{comp}}$  for simplicity. We observe that the resulting gradient for  $\mathcal{R}(\psi)$  is proportional to the noise vector  $\mathbf{v}$  and to the gradient of the estimated RIR  $\hat{\mathbf{h}}(\psi)$  with respect to the parameters  $\psi$ . Therefore, adding  $\mathcal{R}(\psi)$  in the optimization has the result of adding multiplicative noise to the operator gradients (with respect to  $\psi$ ) which emerge from the optimization of the reconstruction loss  $\mathcal{C}(\mathbf{y}, \mathcal{A}_{\psi}(\mathbf{x}_0))$ .

Empirically, this has the effect of smoothing out the optimization of the RIR operator parameters  $\psi$  and avoiding degenerate solutions, provided that the dedicated noise schedule  $\sigma'$  is reasonably chosen.

## C. Experimental details

## 1) Speech Dereverberation:

a) *Architecture and training hyperparameters:* We train the unconditional score model  $\mathbf{s}_{\theta}$  for our method BUDDy with anechoic data only, using segments of 4 seconds randomly extracted from the utterances in VCTK. Same as in [26], [40], we implement the unconditional score network architecture with NCSN++M [25], [55], a lighter variant of the NCSN++ [23] with 27.8M parameters. Similar to [47], we wrap up the network with a time-frequency transform, in this case the STFT, such that the NCSN++M forward pass is effectively performed in the complex STFT domain using a real and imaginary parts representation. For all methods, STFTs are computed using a Hann window of 32 ms and a hop size of 8 ms. The complex prediction at every state can be converted to time-domain by inverting the STFT. We adopt Adam [91] as the optimizer to train the unconditional score model, with a learning rate of  $10^{-4}$  and an effective batch size of 16 for 200k iterations. We track an exponential moving average of the DNN weights with a decay of 0.999 to be used for sampling as in [24].

b) *Baselines:* For WPE [7], we take 5 iterations, a filter length of 50 STFT frames (400ms) and a delay of 2 STFT frames (16ms). We set the hyperparameters of the method by Yohena and Yatabe [8] to  $M = 50$  and  $\rho = 400$  after conducting a parameter search. Using code gently provided by the authors, we retrain Saito et al. [34] and GibbsDDRM [35] using the same data as for BUDDy, i.e. the anechoic VCTK dataset. We use the same inference parameters which can be found in [34], [35] although we tried to improve the results by doing a hyperparameter search as suggested by the authors. We re-train RVAE-EM in unsupervised mode on our anechoic VCTK dataset using publicly available code and use the original inference parameters reported by the authors [38].

c) *Reverberation operator:* The STFT parameters are the same as those used in the unconditional score model, i.e. we use a Hann window of 32 ms and a hop size of 8 ms. For subband filtering we further employ 50% zero-padding to avoid frequency aliasing artifacts. Given our sampling rate of  $f_s = 16$  kHz, this results in  $K = 513$  unique frequency bins. We set the number of STFT frames of our operator to  $N_{\mathbf{h}} = 100$  (800ms). We subsample the frequency scale in  $B = 26$  bands, with a 125 Hz spacing between 0 and 1kHz, a 250Hz spacing between 1 and 2kHz, and a 500Hz spacing between 3 and 8kHz.

We optimize the RIR parameters  $\psi$  using Adam, with a learning rate of 0.1, and the momentum parameters are set to  $\beta_1 = 0.9$ , and  $\beta_2 = 0.99$ . We employ  $N_{\text{its.}} = 10$  optimization iterations per diffusion step. We further constrain the weights  $w_b$  between 0 and 40 dB, and the decays  $\alpha_b$  between 0.5 and 28. This avoids the optimization from approaching degenerate solutions, especially at the early stages of sampling.

d) *Forward and reverse diffusion:* As mentioned in Section IV-B we obtain our initial estimate  $\mathbf{x}_{\text{init}}$  through WPE dereverberation. Consequently, we choose  $T = 0.5$  such that the initial noise in  $\mathbf{x}_T \sim \mathcal{N}(\mathbf{x}_{\text{init}}, \sigma^2(T)\mathbf{I})$  effectively masks potential artifacts stemming from WPE, while still retaining the general structure in  $\mathbf{x}_{\text{init}}$  that may guide the process. We



set the minimal diffusion time to  $T_{\min} = 10^{-4}$  and adopt the same reverse discretization scheme as Karras et al. [44]:

$$\forall i < N, \tau_i = \sigma_i = \left( T^{1/\rho} + \frac{i}{N-1}(T_{\min}^{1/\rho} - T^{1/\rho}) \right)^\rho, \quad (21)$$

with warping  $\rho = 10$  and  $N = 200$  steps. We use the second-order Euler-Heun stochastic sampler in [44] with  $S_{\text{churn}} = 50$ . In the noise regularization term depicted in (16), the annealing schedule  $\sigma'$  follows the same discretization as  $\sigma$ , but we restrict its values between  $\sigma'_{\min} = 5 \times 10^{-4}$  and  $\sigma'_{\max} = 10^{-2}$ . The scaling factor used for the variance estimate  $\eta(\tau)$  in (9) is fixed to  $\tilde{\eta} = 0.6$ .

*e) Listening experiment:* We conduct a listening experiment based on the MUSHRA recommendation [74] using the webMUSHRA<sup>3</sup> interface. The test comprised 12 pages, featuring 6 reverberant speech utterances from each of the *matched* and *mismatched* datasets. The test was conducted in isolated conditions within listening booths at the Aalto Acoustics Lab. In total, 10 volunteers participated in the experiment. All utterances were loudness-normalized to -23dB LUFS. The participants were allowed to modify the volume of headphones during the training stage (first page, not included in the results). The ground-truth anechoic speech served as the reference, which was also hidden among the other conditions (WPE, RVAE-EM, PSE, SGMSE, BUDDy), while the original reverberant speech signal was used as the low anchor, expected to receive a score of 0. Participants were advised to focus particularly on dereverberation performance and to use the full rating scale, i.e. rate reference as 100 and reverberant anchor as 0. We obtained consent directly from the participants through a written form. As the study did not present any risk for the subjects, no review board was required for the approval of this experiment.

## 2) Singing Voice Dereverberation:

We use the UNet architecture proposed in [84] without self-attention blocks, and wrap the computations within an invertible Constant-Q Transform (CQT) [85]. The resulting architecture consists of 45M parameters. We employ a 1534-point window and hop size 384 for the CQT. The unconditional score model is optimized using Adam with same parameters as for the VCTK dataset, but we reduce the batch size to 4 and use 6-second anechoic audio segments. For this experiment, we use  $B = 39$  bands for the subband decomposition in the reverberation operator for BUDDy, extending the bands used in Appendix C1c above 8kHz with a 1kHz spacing.

<sup>3</sup><https://github.com/audiolabs/webMUSHRA>